Egypt. J. Chem. **Vol. 68**, No. 2 pp. 27 - 37 (2025)

Egyptian Journal of Chemistry

http://ejchem.journals.ekb.eg/

Effect of deposition of Al_2O_3 as interdiffusion barrier on the microstructure and optical properties of Ti thin film.

Hanan Abd El-Fattah[a], Aliaa Abdelfatah[b], Iman Elmahallawi[b,c], Ahmed Ibrahim[d], Lamiaa Z. Mohamed[b,*]

[a] *Department of Manufacturing Engineering and Production Technology, Modern Academy for Engineering and Technology, Cairo, Egypt*

[b] *Mining, Petroleum, and Metallurgical Engineering Department, Faculty of Engineering, Cairo University, Giza, 12613, Egypt*

[c] *The Centre for Renewable Energy, The British University in Egypt, El Shorouk, Cairo, Egypt*

[d] *Faculty of Postgraduate Studies for Nanotechnology, Cairo University, Egypt*

Abstract

In this work, magnetron sputtered Ti and Al2O3/Ti have been investigated. Microstructure, morphology, phase identification, mechanical, and optical properties were studied. Heat treatment at 600◦ C for 2h with different cooling rates was applied. X-ray diffraction (XRD) was used in phase and structure identification. Scanning electron microscopy (SEM) and atomic force microscopy (AFM) were used for microstructure and morphology investigations. Microhardness is used for mechanical properties measurements. The FTIR and spectrophotometry were used for optical characterizations. It was found that the Al2O3/Ti structure has a higher hardness value at all conditions compared to Ti. Resulted in TiO2 phases after heat treatment varying due to the cooling rate. As deposited Al2O3/Ti structure has the highest selectivity value (absorbance/emittance). Al2O3/Ti structure has a higher selectivity value at all conditions than Ti.

Keywords: Phase vapor deposition; Thin film; Selective absorber; Titanium; Aluminum oxide; Thermal solar energy

1. Introduction

Solar-selective absorbance properties refer to the ability of a material or surface to selectively absorb solar radiation while minimizing the absorption of other wavelengths [1]. This property is desirable in various applications, such as solar thermal collectors, photovoltaic cells, and solar coatings for windows and building materials [2]. In solar thermal collectors, the goal is to maximize the absorption of sunlight in the visible and near-infrared range (0.3 to 2.5 micrometers) while minimizing the absorption of thermal radiation in the mid-infrared range (2.5 to 25 micrometers). This is achieved by using materials with high solar absorbance and low thermal emittance [3]. Solar absorbance is a measure of how well a material absorbs solar radiation, while thermal emittance is a measure of how well a material emits thermal radiation [4]. Selective absorber materials are typically designed to have a high absorption coefficient in the solar spectrum range (0.3 to 1.1 micrometers), which corresponds to the wavelengths of maximum solar radiation. This allows the receiver to absorb a large portion of the incident solar energy [5]. At the same time, the material should have a low emittance in the long infrared range (beyond 2.5 micrometers) [6]. Solar coatings for windows and building materials aim to control the amount of solar radiation that enters a building. These coatings are often designed to have high solar reflectance (R) and low solar absorbance to minimize heat gain from solar radiation. By reflecting a significant portion of the incident solar energy, these coatings can help reduce the cooling load on buildings and improve energy efficiency [7]. Various materials and surface treatments can be used to achieve solar-selective absorbance properties. For example, selective coatings can be applied to surfaces to enhance their solar-absorbing or reflecting properties. These coatings often consist of multiple layers of materials with different optical properties, such as metals, semiconductors, and dielectrics. The specific design of the coating determines its solar-selective properties [8]. Overall, solar-selective absorbance properties are crucial for optimizing the performance and efficiency of solar energy conversion devices, as well as for controlling heat gain in buildings exposed to sunlight [9]. Research in this field continues to explore new materials and technologies to improve solar absorbance and reduce thermal emittance for various applications [10]. Thin films play a crucial role in the manufacturing of solar cells and plants. They are used to create the active layers that absorb sunlight and convert it into electricity [9]. It's important to note that the specific application of thin films in

*Corresponding author e-mail: lamiaa.zaky@cu.edu.eg ; (Lamiaa Z. Mohamed).

Receive Date: 07 March 2024, Revise Date: 02 June 2024, Accept Date: 23 June 2024

DOI: 10.21608/ejchem.2024.275380.9420

thermal solar energy technology may vary depending on the type of receiver and the desired performance characteristics. The choice of materials and thin film deposition techniques can also impact the efficiency and functionality of the receiver in thermal solar energy [11]. Alumina is an effective dielectric material that reduces reflection of solar radiation and alumina-based cermet is good at absorbing solar radiation. Alumina-based solar selective coatings have superior optical properties [12]. Titanium dioxide (TiO_2) has many excellent properties in optics, electricity, chemistry, and structure. It has been widely used in optical thin films, photocatalysis, transparent electrodes, sensor applications, protective films, etc. In the field of optical coating, TiO_2 film exhibits good absorbance compared to other oxide materials [13]. TiO_2–Al_2O_3 structures are used in various applications including catalysis, solar cells, photocatalytic, thermal solar energy, and self-cleaning [14, 15]. Several methods have been used to prepare TiO_2–Al_2O_3 nanocomposites such as the plasma-sprayed method, metalorganic chemical vapor deposition (MOCVD), and sol-gel deposition [16]. Magnetron sputtering and solution chemical methods are commonly used to prepare alumina-based solar selective coatings. However, both techniques have drawbacks. In magnetron sputtering, alumina is typically deposited using radio frequency (RF) sputtering, which has a slower deposition rate and higher equipment cost compared to direct current (DC) sputtering. [17,18]. The sputtering technique can be applied to various substrates, including 304LSS. It is versatile enough for both small-scale research and large-scale industrial production [19]. Researchers are highly interested in producing alumina thin films to provide shielding for substrates made of metallic and other materials [20]. Researchers have paid great attention to TiO_2, Al_2O_3, and TiN_xO_y thin films for thermal solar energy selective absorbers. The authors have successfully obtained oxide thin films TiO_2 by oxidation of TiN at 800˚C for 2 hrs [21], TiO_2 & Al_2O_3 by oxidizing Ti & Al thin films at 400˚C and 800°C [14]. The microstructure and optical properties of the formed oxides were studied at different temperatures and compared with those of the sputtered thin films [21]. The previous work by the authors [14, 21] has shown that the route of sputtering of thin metallic films of Ti and Al followed by annealing is beneficial for tailoring multi-layered coatings for selective solar absorbers requiring graded high absorbance and low emittance materials. The results also showed the formed microstructures have a significant effect on the optical properties of the thin films deposited on the surfaces. This work is designed based on the previous results showing that after oxidation Ti thin film has higher absorbance, compared to Al, while the Al thin film has lower emittance, suggesting that building multilayers of TiO_2 and Al_2O_3 thin films is worth investigating. Therefore, the main aim of this work is to investigate the effect of using Al_2O_3 as an interlayer below the TiO_2 thin film produced via the annealing route of sputtered Ti. In this work, annealing is conducted at a Temperature (600˚C) for oxidizing Al and Ti thin films to avoid the negative effect of oxidizing at 800C and to optimize the effect of oxidizing temperature on the optical properties and microstructure of formed oxides to achieve a good selective absorber for high temperature solar thermal applications. Ti thin film was deposited by physical vapor deposition (PVD) in this work. After deposition, Ti was heat treated at 600˚ C with different cooling rates to have TiO_2. In this work, the effect of the Al_2O_3 layer deposited in between Ti thin film and substrate has been investigated. The Ti thin film was deposited directly above the substrate (structure 1) and deposited above Al_2O_3 (structure 2). The microstructure, morphology, microhardness, and optical properties of both structures have been studied before and after heat treatment. The effect of Al_2O_3 deposition as an interlayer will be discussed. The absorbance pattern became different in structure 2 as the presence of the Al_2O_3, especially after heat treatment, resulted in changes in the absorbance pattern and the microhardness in structure 2.

2. Experimental work

2.1 Thin film deposition

Deposition of thin film occurred by PVD sputtering technique. Two pure targets of Al_2O_3 and Ti with a percentage of about 99.9% were used in deposition. Only Ar gas was used in deposition with a 30 Sccm flow rate. 304 L stainless steel (SS) substrates were cleaned and dried before being fixed in the chamber. Power, pressure, and temperature were used in sputtering are 1.15 kW, 10^{-3} pa, and 160˚ C respectively. Each layer was deposited in time about 60 min.

2.2 Heat treatment process

Two thin film structures shown in Figure 1 are heat treated at 600˚C for 2h but the cooling rate was changed. Structure 1 consists of 304 LSS as substrate and Ti thin film deposited above it. Structure 2 consists of 304 LSS as substrate, Al_2O_3 deposited above it, and Ti thin film deposited in the top. The main purpose of changing the cooling rate is to study the effect of it on the microstructure and optical properties of deposited thin films. Half of the specimens were left to cool in the furnace (annealing) and the other half was cooled in air (normalizing).

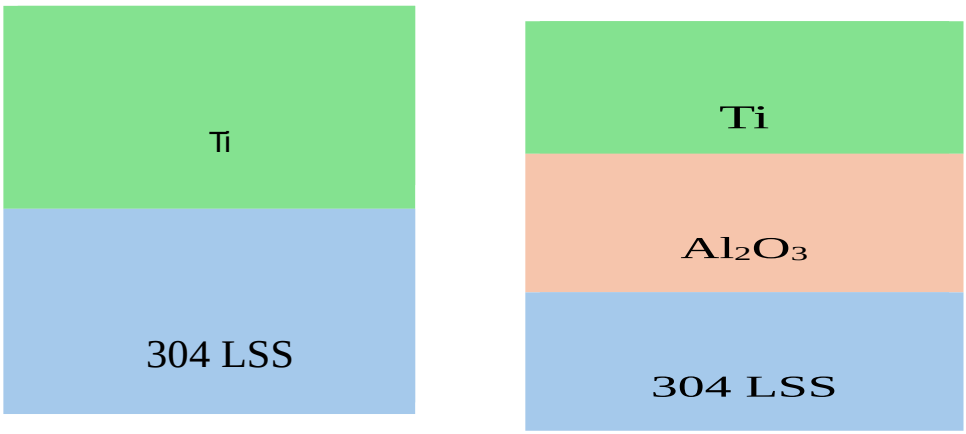

Structure 1 Structure 2

Figure 1 Schematic drawing for two deposited structures.

2.3 Thin film characterization

SEM was used first to investigate the surface microstructure. FEI inspect S- Netherlands equipment was used. Roughness and morphology before and after heat treatment were measured by the AFM 5600LS version. The phases and structure of thin films were explained by the XRD Burker model with Cu target. For optical properties spectrophotometer and FTIR equipment were used. Also, the microhardness test with HV0.5 (4.903N)- 10- Sec was applied to explain the differences in the two structures and the effect of the presence of Al_2O_3.

3. Results and discussions

3.1 Phase Identification (XRD)

Figure 2 shows the XRD patterns of structure 1 with and without heat treatment at 600° C for 2 h. Cooling in the furnace or air after heat treatment is also illustrated in Fig. 2. Fig.3 represents the XRD patterns of structure 2 before and after heat treatment at 600° C for 2 h then cooled in the furnace or air. Ti thin film in two structures was oxidized and formed TiO_2. In Figs 2 and 3 and other figures in the paper letters A and F in the figs mean cooling in air and cooling in a furnace respectively. Table 1 depicts each condition with phases and peak angles. The results in the case of deposited thin films in structures 1 and 2 confirmed the formation and presence of Ti and Al_2O_3. After heat treatment of the two structures followed by air cooling anatase TiO_2 was only found. Moreover, results indicate the furnace cooling resulted in anatase and rutile TiO_2 phases. In general, the band gap of TiO_2 is larger than 3 eV which makes pure TiO_2 active for UV light. The difference between anatase and rutile is the width of the band gap of each one which is 3.2 eV for anatase and 3.0 eV for rutile [22]. In the case of air cooling after heat treatment, no rutile diffraction peaks were observed. The rutile phase didn't appear in both structures because of air cooling being fast and not allowing equilibrium phases to appear. The wide or narrow band gap of TiO_2 anatase or rutile phases has a direct effect on the optical properties, as will be shown later.

Table 1 XRD phases and planes at all conditions

Condition	Phase	Peaks angle	Phase plane	Anatase(N) or Rutile (R)	Ref.
304LSS/Ti	Ti	36.2, 39, 42.5, 52.4	(101), (002), (101), (211)	-	[23]
304LSS/Ti-A	TiO_2	35.8, 39, 46, 51.9	(004), (111), (200), (211)	N, N, N, N	[23, 24, 25]
304LSS/Ti-F	TiO_2	39, 52, 68	(111), (211), (301)	N, N, R	[23, 24, 25, 26]
304LSS/Al2O3/Ti	Ti & Al_2O_3	39.5, 44, 51	(101), (113), (024)	-	[23, 27]
304LSS/Al2O3/Ti-A	TiO_2 &Al_2O_3	39, 44, 52	(111), (113), (211)	N, -, N	[23, 27]
304LSS/Al2O3/Ti-F	TiO_2 &Al_2O_3	37, 39, 42, 44, 46, 52	(101), (111), -, (113), (200), (211)	R, N, R, -, N, N	[23, 26, 27]

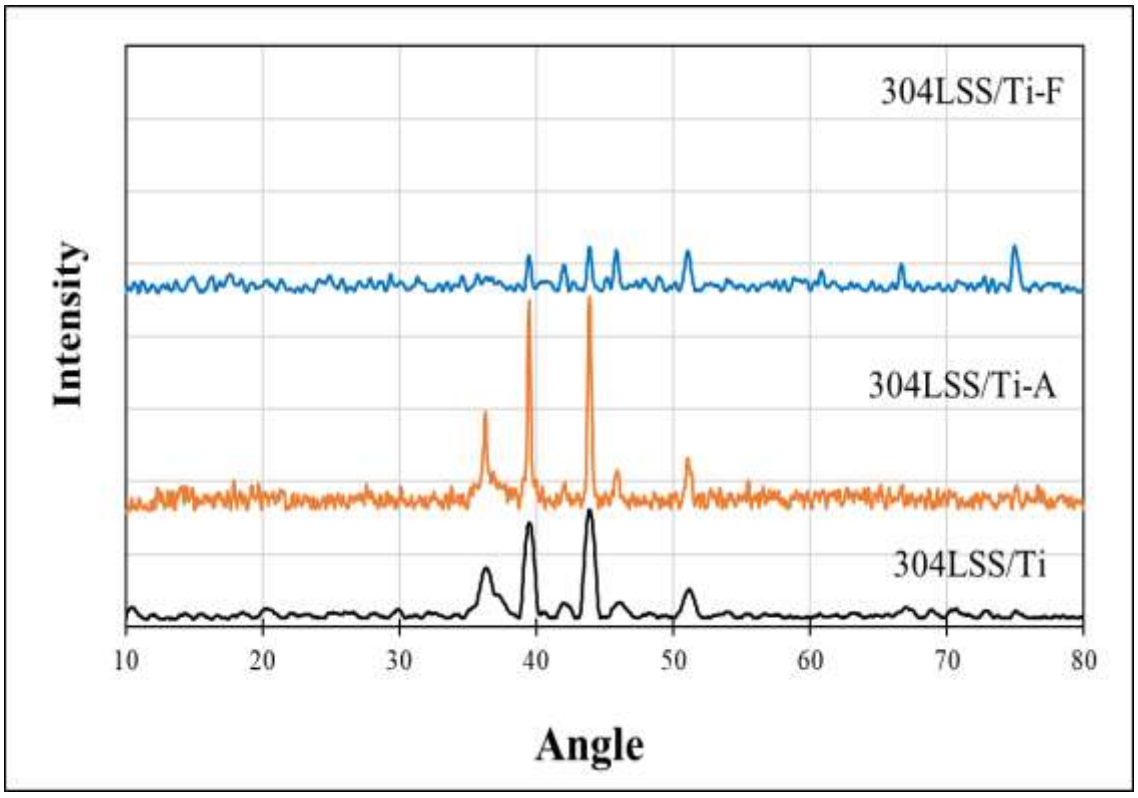

Fig. 2. The XRD patterns of structure 1 before and after heat treatment.

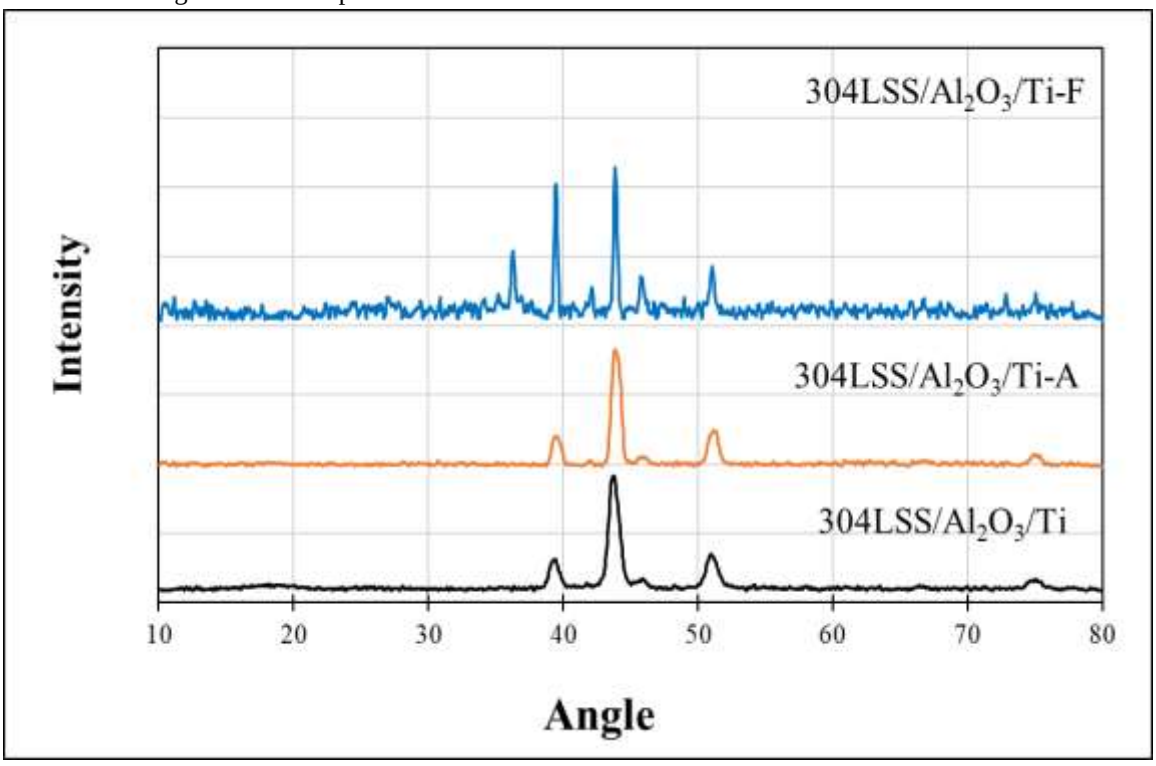

Fig. 3. The XRD patterns of structure 2 before and after heat treatment.

3.2 Microstructure (SEM) & surface morphology (AFM)

Figure 4 shows the SEM image of structures 1 & 2 after heat treatment in the furnace at 600° C for 2 h and then cooled in the furnace. TiO_2 formed after annealing in two images Figs. 4 a and b have two different microstructures. The effect of Al_2O_3 presence as an interlayer in structure 2 on the microstructure is found clearly. Fig 4 a represents the TiO2 microstructure formed in structure 1, as the thin film was detailed cracks and holes appeared. In Fig 4 b microstructure of TiO_2 in structure 2 is homogenous without any cracks, holes, or deterioration. The Al_2O_3 interlayer in structure 2 prevented the diffusion from SS substrate to Ti thin film at high temperatures due to the stability of Al_2O_3 at elevated temperatures. Interdiffusion barriers are used between substrates and coating to reduce the degradation of coating at high temperatures by reducing the Ti losses to the substrate [28]. Substrate elements such as Cr and Ni found in SS diffused into the coating and increased its ability to degrade, corrosion, and oxidation resistance [28]. Al_2O_3 played an important role as an interdiffusion barrier in the prevention of the SS elements diffusing inside the Ti thin film which resulted in a homogenous TiO_2 microstructure.

Figure 5 illustrates the AFM images of two structures at all conditions. Table 2 explains the roughness (Ra) and root mean square (RMS) measurements of the surface of two structures at all conditions. RMS roughness is distinct from the amounts of roughness profiles that are located away from the midline [29]. RMS is the standard deviation of the mean height Z [30], calculated mathematically by equation (1). N is the number of peaks; Z is the mean height of N peaks, and Z_N is the height of each peak

$$\text{RMS} = \sqrt{\frac{\sum_{N=1}^{N}(Z_N - Z)^2}{N-1}} \quad (1)$$

As mentioned in Table 2 roughness decreased after heat treatment. Furthermore, roughness has the lowest value after furnace cooling in two structures. The roughness of as deposited Ti thin film in Structure 2 is lower than as deposited Ti in Structure 1. The roughness of Ti decreased on structure 2 because it is deposited on the Al_2O_3 thin film, not on the SS substrate directly. Fig. 5 b and c show the Ti thin film after heat treatment and cooling in air and furnace respectively, as shown the formed TiO_2 morphology is similar otherwise the roughness is decreased in case of furnace cooling. Fig 5F presents the columnar structure of formed TiO_2 after heat treatment and furnace cooling [31].

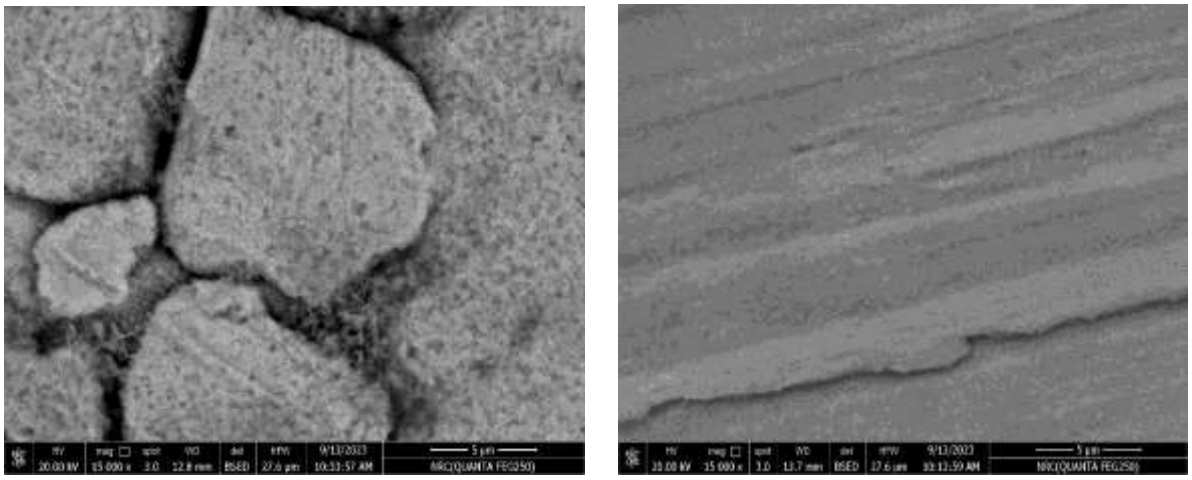

(a) (b)

Figure 4. The two structures after heat treatment at 600° C for 2 h with furnace cooling rate (a) 304L/Ti-F, and (b) 304LSS/Al2O3/Ti-F

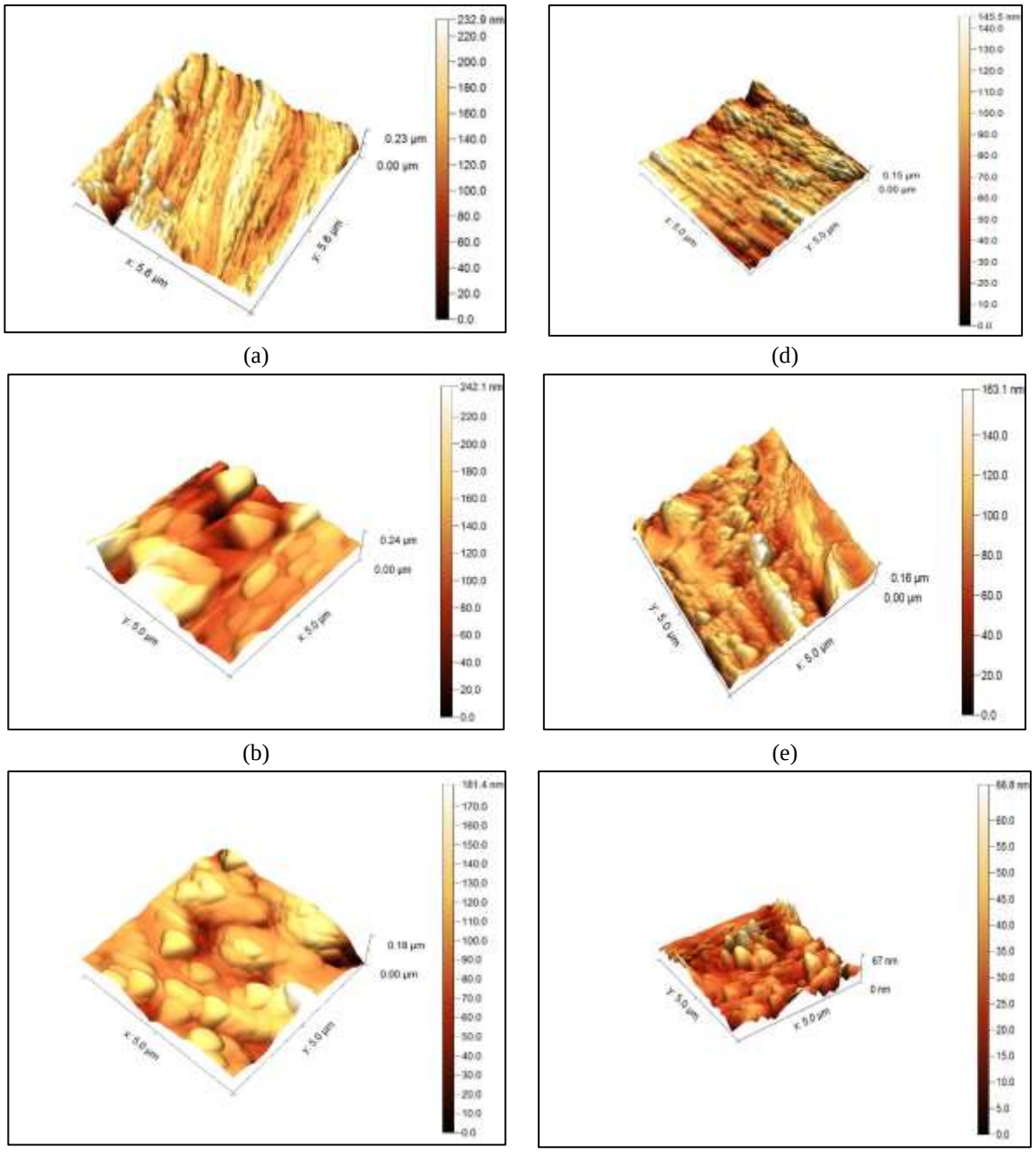

Fig. 5. AFM images for (a) 304LSS/Ti, (b) 304LSS/Ti-600 °C-2h-A, (c) 304L/Ti-600 °C-2h-F, (d) 304LSS/Al_2O_3/Ti, (e) 304LSS/Al_2O_3/Ti-600 °C-2h-A, and (f) 304LSS/Al_2O_3/Ti-600 °C-2h-F

Table 2. The Ra of the different conditions

Condition	Ra, nm	RMS, nm
304LSS/Ti	32.37	40.43
304LSS/Ti-A	28.47	36.5
304LSS/Ti-F	15.40	21.01
304LSS/Al_2O_3/Ti	13.60	17.93
304LSS/Al_2O_3/Ti-A	13.77	18.09
304LSS/Al_2O_3/Ti-F	6.27	8.37

3.3 Microhardness test

The microhardness test was conducted for all conditions. Figure 6 depicts the statistics of microhardness results. The main purpose of applying the microhardness test is to express the effect of the Al_2O_3 layer in Structure 2. The results indicate that values of microhardness of structure 2 are higher than structure 1 in all conditions before and after heat treatment. Increasing the microhardness values in structure 2 confirms the presence of Al_2O_3 and enhances the ability of this structure against degradation.

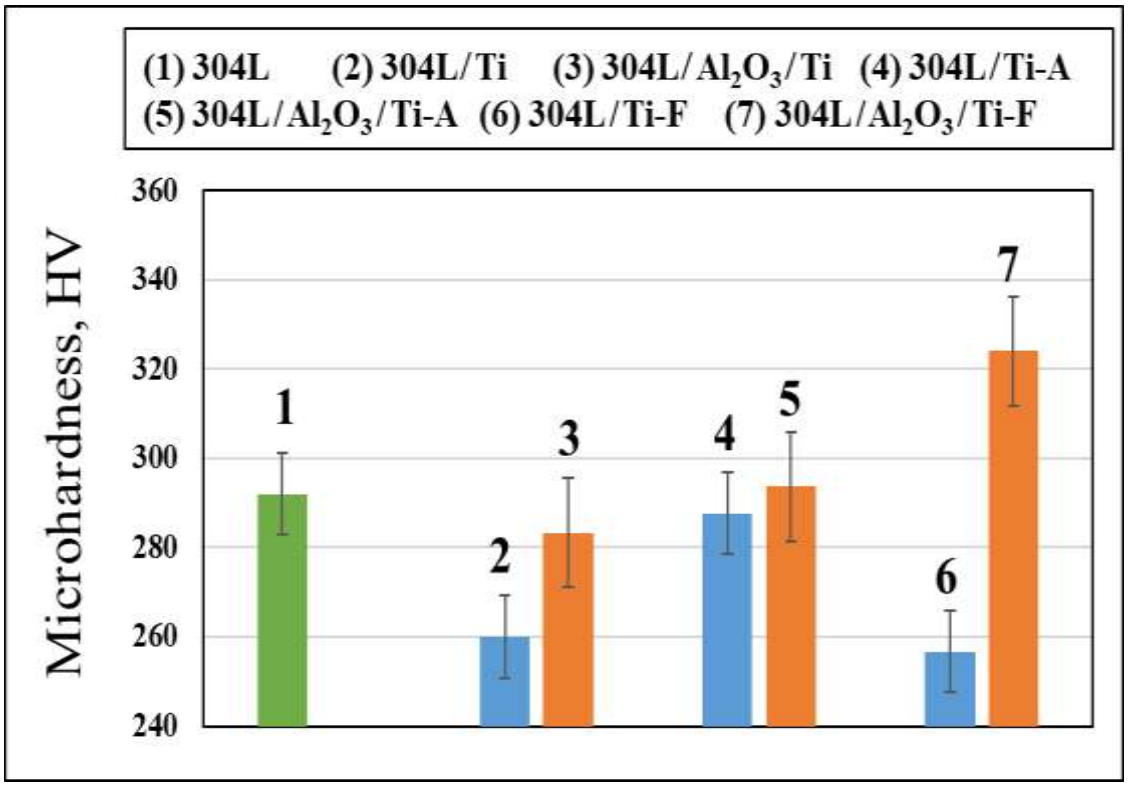

Figure 6. Statistics of microhardness results

3.4 Optical properties

Figures 7, 8, 9, and 10 show the absorbance and emittance curves for structures 1 & 2. Table 3 expresses the selectivity of all conditions. As shown in Figs 7 and 9 the absorbance of the TiO_2 thin film formed after furnace cooling in structure 1 and the TiO_2 resulting from air cooling in structure 2 have the highest absorbance values of all conditions. The highest absorbance value of TiO_2 achieved in both structures is about 92% but the selectivity is different for both conditions, due to the difference in emittance. Selectivity can be defined as absorbance/emittance, and it is used to detect the efficiency of the selective absorber. The selectivity of TiO_2 air-cooled in Structure 2 is higher than the selectivity of TiO_2 in Structure 1 for the furnace-cooled Structure 1. The highest selectivity value of all conditions is for the as-deposited structure 2 (304SSL/Al_2O_3/Ti). Also, all conditions of Structure 2 have higher selectivity values than Structure 1. The deposition of Al_2O_3 as an interdiffusion barrier in structure 2 has a good and positive effect on the selectivity properties of Ti thin film at all conditions.

Eessaa et al prepared a Cu-TiO_2 composite by powder metallurgy [32]. Optical properties were investigated with the different percentages of impeded TiO_2 [32]. They found the composite with the highest percentage of TiO_2 (about 40%) had the highest reflectance which means lowest absorbance [32]. As discussed before in the phase identification section the formed TiO_2 has two phases anatase and rutile phase. Due to the narrow band gap of the rutile phase than anatase so, it can absorb a larger amount of light than the anatase [33]. Furthermore, the anatase phase acts as UV- light harvester because of its wide UV absorption range [34]. As shown in Table 1, the rutile phase appeared in furnace cooling conditions in Structure 1 and Structure 2. The furnace cooling condition in structure 1 has a higher absorbance but structure 2 does not. That's due to roughness which is considered as another factor affecting the absorbance value [35]. Furnace cooling in Structure 2 has the lowest roughness value as shown in Table 2. The lower roughness decreased the absorbance despite the presence of the rutile phase.

Table 3 Selectivity of all conditions (absorbance/ emittance (α/ε))

Condition	Selectivity (α/ε))
304SSL/Ti	0.825/0.091
304SSL/Ti-A	0.89/0.15
304SSL/Ti-F	0.92/0.172
304SSL/Al_2O_3/Ti	0.79/0.051
304SSL/Al_2O_3/Ti-A	0.91/0.147
304SSL/Al_2O_3/Ti-F	0.850/0.102

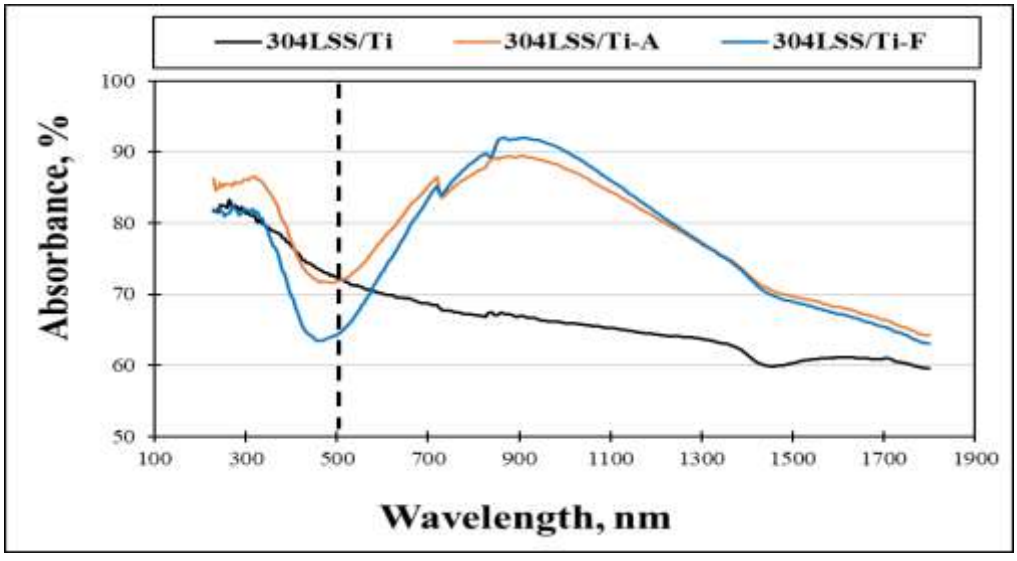

Fig. 7. The absorbance % vs. the wavelength for structure 1 before and after heat treatment.

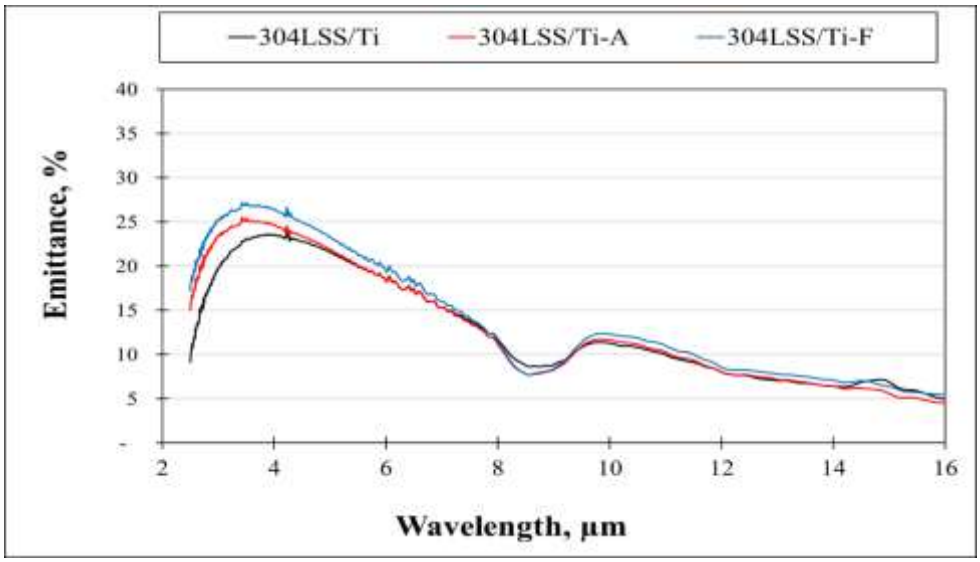

Fig. 8. The emittance % vs. the wavelength for structure 1 before and after heat treatment.

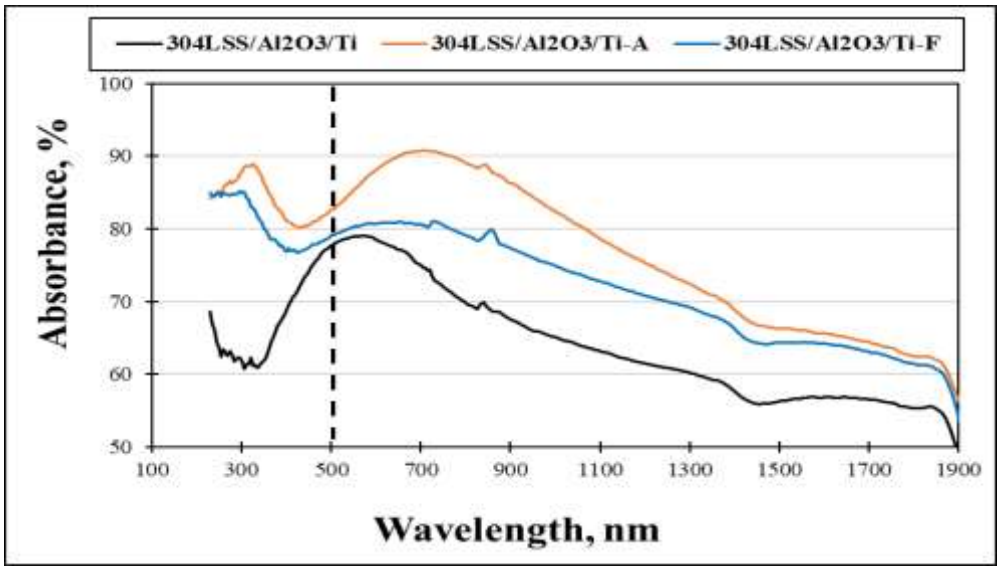

Fig. 9. The absorbance % vs. the wavelength for structure 2 before and after heat treatment.

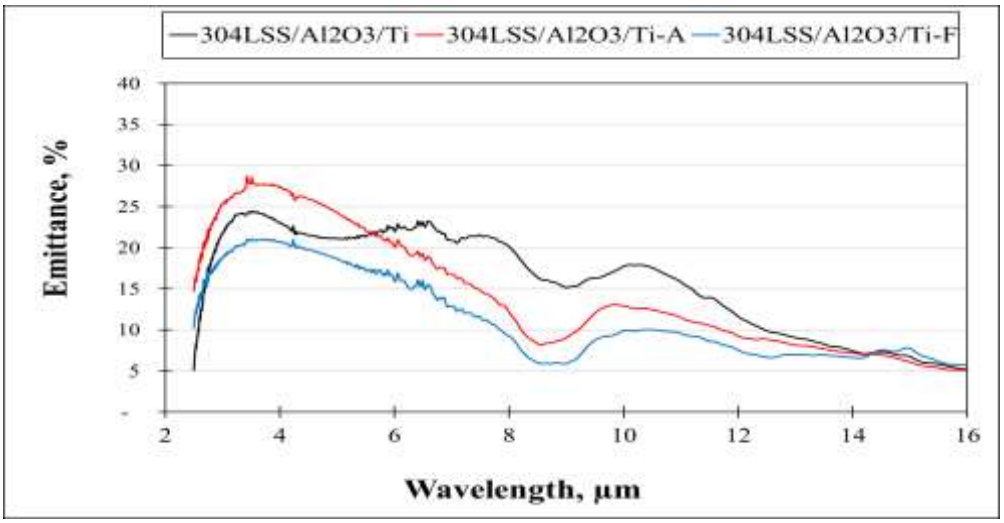

Fig. 10. The emittance % vs. the wavelength for structure 2 before and after heat treatment.

Conclusions

The main purpose of the comparison conducted in this study is to evaluate the effect of the Al_2O_3 layer deposited between Ti and substrate on the structure, morphology, microhardness, and optical properties of Ti before and after heat treatment, where both structures were oxidized at 600° C for 2h and left to cool in different conditions (furnace cooling & air cooling). The study has proven that the thin film structure of 304SSL/Al_2O_3/Ti possesses higher selectivity after air cooling from 600° C for 2h (0.91/0.147) and microhardness (290 HV) compared to the structure of 304SSL/Ti (selectivity 0.89/0.15 after air cooling and microhardness 285 HV). The highest microhardness was achieved for the structure 304SSL/Al_2O_3/Ti (324 HV) after furnace cooling, while the lowest microhardness was achieved for the structure 304SSL/ Ti (255 HV) after furnace cooling.

Conflict of interest

The authors declare that they have no conflicts of interest.

Data Availability

The data will be made available on reasonable request.

Acknowledgment

The authors express their gratitude to the Cairo University Research Support Program for Renewable Energy for providing financial support. Additionally, they extend their appreciation to the Faculty of Engineering and the Faculty of Postgraduate Studies for Nanotechnology at Cairo University, Egypt.

References

1. M. Hu, G.Pei, L. Li, R. Zheng, J. Li, J. Ji, Theoretical and Experimental Study of Spectral Selectivity Surface for Both Solar Heating and Radiative Cooling, International Journal of Photoenergy, (2015) 807875.
2. A. Syafiq, V. Balakrishnan, M.S. Ali, S.J. Dhoble, N.Abd Rahim, A. Omar, A.Abu Bakar, Application of transparent self-cleaning coating for photovoltaic panel: a review, Current Opinion in Chemical Engineering, 36 (2022), 100801
3. J. Zhang, C. Wang, J. Shi, D. Wei, H. Zhao, C. Ma, Solar Selective Absorber for Emerging Sustainable Applications, Advanced Energy and Sustainability Research, (2022)
4. L.A. Omeiza, M. Abid, A. Dhanasekaran, Y. Subramanian, V.Raj, K. Kozak, U. Mamudu, A.K. Azad, Application of solar thermal collectors for energy consumption in public buildings – An updated technical review, J. Eng. Res., (2023)
5. J. Pastuszak, P. Węgierek, Photovoltaic Cell Generations and Current Research Directions for Their Development, Materials (Basel). (2022) 15(16): 5542.
6. S. Akhil, S. Akash, Altaf Pasha, Bhakti Kulkarni, Mohammed Jalalah, Mabkhoot Alsaiari, Farid A. Harraz, R Geetha Balakrishna, Review on perovskite silicon tandem solar cells: Status and prospects 2T, 3T and 4T for real world conditions, Materials & Design, 211(1) (2021) 110138.
7. M.A. Jahid, J. Wang, E. Zhang, Q. Duan, Y. Feng, Energy Savings Potential of Reversible Photothermal Windows with Near Infrared2 Selective Plasmonic Nanofilms, Energy Conversion and Management, 263 (2022) 115705.
8. A.Y. Al-Rabeeah, I. Seres, I. Farkas Selective Absorber Coatings and Technological Advancements in Performance Enhancement for Parabolic Trough Solar Collector, Journal of Thermal Science 31(6) (2022) 1990–2008.
9. J. Zhang, C. Wang, J. Shi, D. Wei, H. Zhao, C. Ma, Solar Selective Absorber for Emerging Sustainable Applications, Advanced Energy and Sustainability Research, (2022)
10. A. Palacios, A. Calderón, C. Barreneche, J. Bertomeu, M. Segarra, A. Inés Fernández, Study on solar absorptance and thermal stability of solid particles materials used as TES at high temperature on different aging stages for CSP applications, Solar Energy Materials and Solar Cells, 201 (2019) 110088.
11. F-D. Lai, W-Y L. Design, Fabrication and Analysis for Al2O3/Ti/Al2O3 Colored Solar Selective Absorbers for Building Applications Coatings 2022, 12(4), 521.
12. Y. Ning, J. Wang, C. Sun, Z. Hao, B. Xiong, L. Wang, Y. Han, H. Li, Y. Luo, NiCrAlO/Al2O3 solar selective coating prepared by direct current magnetron sputtering and water boiling, Solar Energy Materials and Solar Cells, 219 (2021) 110807.
13. L-S Gao, Q-Y Cai, E-T Hu, Q-Y Zhang, Y-T Yang, Y-B Xiong, B-J. Liu, W-B Duan, T-Y. Yu, D-Q. Liu, Optimization of optical and structural properties of Al2O3/TiO2 nano-laminates deposited by atomic layer deposition for optical coating, Optics Express, 31(8) (2023) 13503.
14. H. Abouarab, I. El-Mahallawi, A. Kassry, H. AbdEl-Fattah, Characteristics of Al & Ti oxide-thin films for thermal solar energy selective absorption applications. Materials Express. 2022, 12, 1–12
15. A. Abdelfatah, L.Z. Mohamed, I. Elmahallawi, H. Abd El-Fattah, Comparison of structure and solar-selective absorbance properties of Al2O3 thin films with Al and Ni reflector interlayers. Chemical Papers. 2023
16. U.O. Akkaya Arıer a, Fatma Zehra Tepehan, Influence of Al2O3:TiO2 ratio on the structural and optical properties of TiO2–Al2O3 nano-composite films produced by sol gel method, Composites Part B: Engineering, 58, 2014, Pages 147-151
17. J.A. García-Valenzuela, R. Rivera, A.B. Morales, Vilches, L.G. Gerling, A. Caballero, J.M. Asensi, C. Voz, J. Bertomeu, J. Andreu, Main properties of Al2O3 thin films deposited by magnetron sputtering of an Al2O3 ceramic target at different radio-frequency power and argon pressure and their passivation effect on p-type c-Si wafers, Thin Solid Films, 619 (2016) 288-296.

18. M.I. Hamil, M.K. Khalaf, M. Al-Shakban, A Study Corrosion Properties by Magnetron Sputtered Nanocrystalline Al2O3 Thin Films, Egypt. J. Chem. 65(11) (2022) 413 – 419.
19. H. Abd El-Fattah, L.Z. Mohamed, I. Elmahallawi, A. Abdelfatah, Corrosion characteristics of Ti and Al2O3/Ti thin films sputtered on 316LSS, International Journal of Electrochemical Science 19 (2024) 100426
20. E.M. Sadek, L.Z. Mohamed, E.F. El-Kashif, A. Abdelfatah, Fabrication and Characterization of Functionally Graded Nanomaterials (Al/Al2O3) and (Al/Ni/Al2O3) using the Sputtering Technique, Egypt. J. Chem. Vol. 67, No. 7 pp. 233 - 249 (2024)
21. H.A. Abd El-Fattah, M.H. Shazly, I.S. ElMahallawi, W.A. Khalifa, Optical properties and microstructure of TiN thin films before and after annealing, Materials Express. 2158-5849, 2019.
22. T. Luttrell, S. Halpegamage, J. Tao, A. Kramer, E. Sutter, M. Batzill, Why is anatase a better photocatalyst than rutile? - Model studies on epitaxial TiO2 films. Scientific Reports, (2014) 4: 4043
23. Q. Du, D. Wei, Y. Wang, S. Cheng, S. Liu, Y. Zhou, D. Jia, The effect of applied voltages on the structure, apatite-inducing ability and antibacterial ability of micro arc oxidation coating formed on titanium surface. Bioactive Materials. 3(2018) 426-433
24. V-T. Nguyen, T-C Cheng, T-H. Fang, M-H. Li, The fabrication and characteristics of hydroxyapatite film grown on titanium alloy Ti-6Al-4V by anodic treatment. Journal of Materials Research and Technology. 9, 3, 2020, 4817-4825
25. M. Chen, M. Wang, H. Yang, X. Wang, D. Tang, J. Jiang, Pre-oxidation of Ti and its diffusion bonding to K9 glass: microstructure and mechanism properties. Metals& Corrosion. J Mater Sci (2022) 57:6790–6802
26. T-H. Koo, J.S. Borah, Z-C. Xing, S-M. Moon, Y. Jeong, I-K. Kang, Immobilization of pamidronic acids on the nanotube surface of titanium discs and their interaction with bone cells. Nanoscale Research Letters 2013, 8:124
27. B.R. Bade, S. Rondiya, S.R. Bhopale, N.Y. Dzade, M.M. Kamble, A. Rokade, M.P. Nasane, M.A. More, S.R. Jadkar, A.M. Funde, Investigation of growth mechanism for highly oriented TiO2 nanorods: the role of reaction time and annealing temperature. SN Applied Sciences (2019) 1:1073.
28. J.A. Haynes, Y. Zhang, K.M. Cooley, L. Walker, K.S. Reeves, B.A. Pint, High-temperature diffusion barriers for protective coatings. Surface and Coatings Technology 188–189, 2004, 153-157
29. A. Bourezgui, I. Kacem, I.B. Assaker, M. Gannouni, J.B. Naceur, M. Karyaoui, R. Chtourou, Synthesis of porous TiO2 thin films prepared with templating technique to improve the photoelectrochemical properties. J Porous Mater (2016) 23:1085–1094
30. D.J. Whitehouse, Handbook of Surface Metrology. Vol. 988. London: IOP Publishing Ltd; 1994.
31. R.T. Bento, M.F. Pillis, Titanium Dioxide Films for Photocatalytic Degradation of Methyl Orange Dye. Titanium Dioxide - Material for a Sustainable Environment. (2018)
32. A.K. Eessaa, O.A. Elkady, A. M. El-Shamy, Powder metallurgy as a perfect technique for preparation of Cu–TiO2 composite by identifying their microstructure and optical properties, Scientific Reports, 13, (2023).
33. M. Batzill, Fundamental aspects of surface engineering of transition metal oxide photocatalysts. Energy Environm. Sci. 4, 3275–3286 (2011).
34. G. Zerjava, K. Zizek, J.Z. snik, A. Pintar, Brookite vs. rutile vs. anatase: What`s behind their various photocatalytic activities? Journal of Environmental Chemical Engineering, 10 (2022) 107722
35. H. Abd El-Fattah, Effect of surface morphology on optical properties of two multilayer structures CuO/ZnO/SiC and Al2O3/ZnO/SiC, Scientific Reports (2023) 13:23035.